# The temperature dependence of the photoluminescence and lifetime of ZnTe:O



1993 J. Phys.: Condens. Matter 5 9235

(http://iopscience.iop.org/0953-8984/5/49/025)

J. Phys.: Condens. Matter 5 (1993) 9235–9252. Printed in the UK

# The temperature dependence of the photoluminescence and lifetime of ZnTe:O

Y Burki†, W Czaja†, V Capozzi‡ and P Schwendimann§

† Institut de Physique Appliquée, EPFL, CH-1015 Lausanne, Switzerland
‡ Dipartimento di Fisica, Università degli Studi di Bari, I-70126 Bari, Italy
§ Defence Technology and Procurement Agency, System Analysis Division, CH-3003 Bern, Switzerland

Received 12 July 1993

**Abstract.** The temperature dependence of the luminescence of the ZnTe:O isoelectronic trap is presented for different excitation energies and is interpreted within a simple model. Interactions that are responsible for the temperature dependence of the lifetime at different excitation energies are discussed.

## 1. Introduction

In this paper we discuss the photoluminescence (PL) of the isoelectronic trap oxygen in ZnTe. Besides their relevance in their own right, its characteristics are related to the gain spectra recently observed for ZnTe:O. In fact, for moderate concentrations of oxygen centres of about $10^{17}$ cm$^{-3}$, a large optical gain has been observed both at 2 K [1] and at room temperature [2] in the spectral region between 0.64 $\mu$m and 0.72 $\mu$m. The data were interpreted within a four-level vibronic laser model, which was derived from a microscopic model [3, 4]. Apart from its potential usefulness for laser applications of ZnTe:O, a study of its optical properties shows a number of interesting results concerning the physics of the material. Bound-exciton luminescence that persists up to room temperature and luminescence with oxygen radiative decay times whose temperature dependence varies with excitation energy are two of the most surprising features observed for this material. As we will show in the following, the analysis of luminescence relies heavily on the formalism already used when discussing luminescence from the isoelectronic trap AgBr:I [5, 6]. The comparison between theory and experiment is satisfying for both traps. This indicates that the model of [5] is suited for the discussion of the optical properties of different isoelectronic traps. We concentrate here on luminescence and on radiative lifetimes of oxygen-bound excitons and their temperature dependence. The features of absorption by ZnTe:O have already been analysed in [7].

In section 2 we give a short account of the experimental arrangement used for the measurements. In section 3 the results on luminescence for both low and high temperatures as well as for resonant and band-to-band excitation are presented and discussed within the model of [5]. In section 4, we discuss the experimental results for the relaxation times measured under the same conditions as mentioned in section 3. Concluding remarks are contained in section 5.

## 2. Experimental details

ZnTe crystals were synthesized from the elements (99.9999% purity) and doped with oxygen in an open system under He gas flow by adding 0.5% ZnO. This doping produces an oxygen concentration of about $10^{17}$ cm$^{-3}$ which seems to correspond to the solubility of oxygen in ZnTe [8]. ZnTe:O is then transported by a mixture of sublimation and chemical transport under Ar pressure with addition of some ZnTe along a temperature gradient from 1100 to 1040 °C and crystals of typical dimensions of 1 cm length with 1 cm diameter are produced.

For PL-integrated intensity and PL-decay-time measurements, ZnTe:O single crystals were mounted on a copper finger of continuous-flow liquid He cryostat equipped with a heat exchange chamber for the samples. To monitor the sample temperature, a calibrated Pt resistor was mounted in the sample holder, next to the crystal. Temperature was measured by means of an automatic resistor bridge and it could be varied from 5 K to room temperature. For measurements at 2 K, samples were immersed in a pumped liquid He bath.

The optical excitation was performed with the continuous wave 478 nm line of an argon-ion laser for excitation into the band edge and with a rhodamine 6G dye laser (pumped by the argon laser), tuned at 587 nm, for resonant excitation within the oxygen absorption band. Neutral density filters were used when necessary to prevent excitation saturation. The emitted light was collected from the front surface of the crystal (at $\pi/2$ with respect to the incident laser beam) and focused on the entrance slit of a 1.5 m focal length scanning spectrometer with a resolution slightly better than 0.5 Å. The signal was detected with a cooled (−20 °C) photomultiplier, and a standard photon-counting system including a PC was used to record and correct data for the spectral response of the detection system.

For PL decay time measurements, the continuous laser beam was pulsed by means of a cavity dumper for both above-mentioned optical excitations. The laser pulses had a fall time of about 9 ns and a repetition rate of 8 kHz (limited by the detection electronics). The emitted light was focused on the entrance slit of a spectrometer (15 cm focal length) used as a 200 nm band-pass. An additional low-pass red filter (cut-off 500 nm) was used before the spectrometer to cut the diffused laser light and the intrinsic PL when exciting into the band edge. The signal was detected by a fast photomultiplier and sampled by a box-car integrator (triggered by the cavity dumper delayed signal), together with a time-scanning module. The PL signal was recorded and analysed by means of a PC.

## 3. Luminescence spectra

In this section we present the luminescence spectra of ZnTe:O from low temperature (2 K) up to room temperature and for band-to-band excitation as well as for excitation into the absorption band of the oxygen isoelectronic trap. In order to stress the peculiarities of the two temperature regimes we present our results in two separate subsections.

### *3.1. Low-temperature luminescence*

We discuss the luminescence spectrum of ZnTe:O within the scheme of the model of Testa *et al* [5], which was first developed for AgBr:I and which allows one to describe the effects of the coupling to both optical and acoustical transverse and longitudinal phonons (TO, TA and LO, LA respectively in the following).

In this model we introduce the experimental one-phonon density of states obtained from calculations and a fit of neutron scattering data. The phonon density of states is divided into four different regions, each of them consisting approximately of a one-phonon mode. The

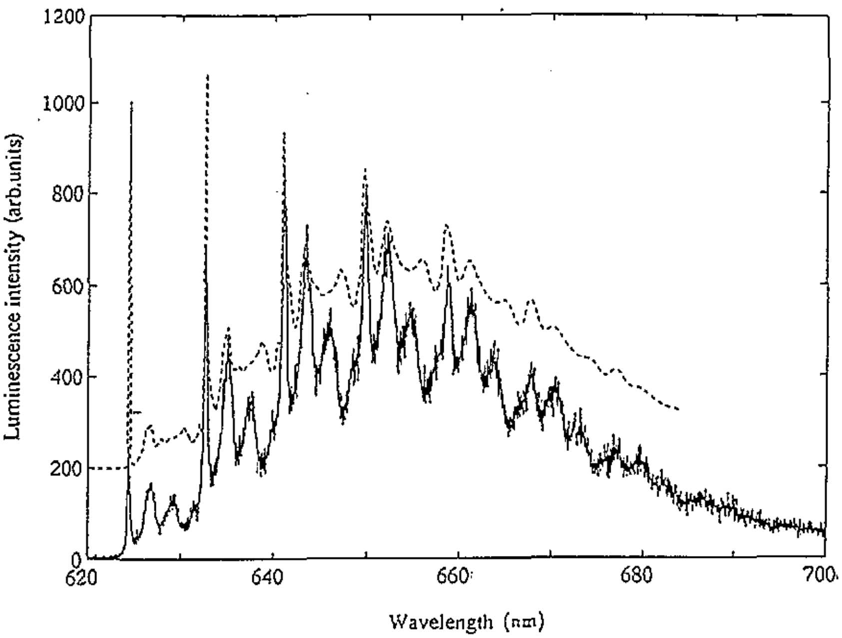


**Figure 1.** Experimental (solid line) and fitted (dotted line) luminescence spectra at 2 K.

coupling strength is then set for each mode for the best fit of the luminescence spectrum. The result is shown in figure 1.

This model thus allows a more exhaustive interpretation of the fine structure observed in the luminescence spectrum when compared with the ones proposed by Dietz *et al* [9] and Hjalmarson *et al* [10]. The result of the fit is rather satisfying as it is shown in figure 1. However, we have to stress the fact that, in spite of the good agreement with experiment, the model of [5] gives only an approximate description of ZnTe:O. In fact, according to group theory, only phonons with $k = 0$ can couple to the electronic transitions. Thus, LO and TO phonons are allowed in one-phonon processes, whereas acoustic phonons can only assist in combinations of at least two whose total momentum vanishes. Since the optical phonon branches in ZnTe are rather flat, a large manifold of combinations of optical with acoustic phonons are possible and are responsible for the temperature dependence. The condition $k_{\mathrm{total}} = 0$ appears in our case as an additional complication to the model [5], which is otherwise well suited for calculating intensities, and in particular their temperature dependence, as shown in figure 3. The introduction of this condition into the model [5] is not obvious and is not the purpose of this paper. Therefore, we have adopted the following approximation: the optical one-phonon and multiphonon repetitions and their temperature dependences are treated within the model of Testa *et al* [5]. Furthermore, in order to simplify calculations, the contributions of the acoustical phonons and their temperature dependence are calculated disregarding the selection rule $k_{\mathrm{total}} = 0$ and using one-phonon density of states in full. This rather crude approximation may account for the differences between the experimental curve and the fit of the acoustical phonons which appears in figure 1.

In order to fit the luminescence spectrum, an energy scaling factor has been introduced, which is most probably related to the dominant electron–LO-phonon coupling which is not included in the density-of-states calculations. It can be seen by inspection of the phonon dispersion curves that LO phonons from point Γ that couple to this transition are those of the extreme edge of the one-phonon density of states, some 3 meV higher in energy than the dominant LO peak. This is exactly the difference between the measured and fitted luminescence spectra.

In most samples tested, a small shoulder next to the zero-phonon line (ZPL) and its LO replica is observed in luminescence while it is not in absorption. This shoulder is known in the literature as the undulation spectrum [11] (see also section 4).

In figure 2 we show the full width at half-height (FWHH) of the ZPL and its LO phonon replicas for emission spectra. In the luminescence spectrum, the small shoulder of the ZPL and its LO replicas mentioned above had to be subtracted in order to obtain a linear dependence on $n$. It is shown in figure 2 that FWHH $\sim n$; this is known to hold also for the case of AgBr:I. It has been shown by Marquis [12] that this behaviour for a LO mode is followed exactly for a one-phonon density of states given by a sum of Lorentzians.

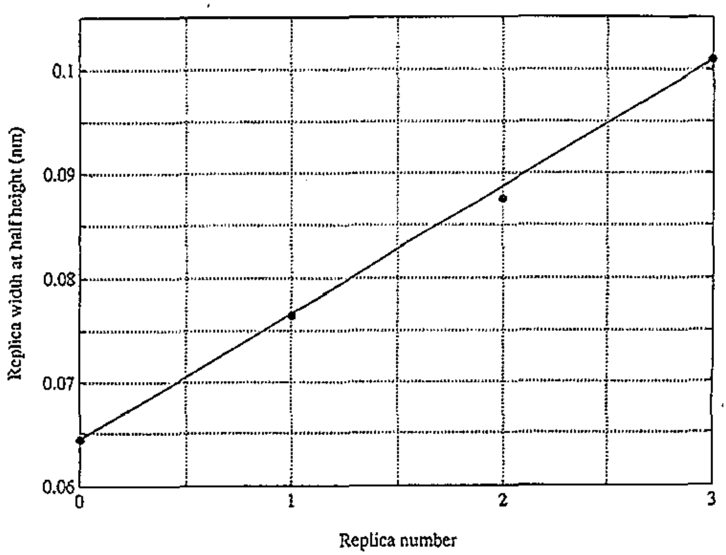


**Figure 2.** The full width at half-height of the ZPL for luminescence.

Furthermore, a few additional observations can be added regarding the general features of figure 1. First, at very low temperature, the occupancy of the energetically higher A state rapidly thermalizes to the lower B state for $kT \leqslant 19$ K.

Only the B line is observed in the luminescence spectrum at temperature lower than $\simeq$ 19 K although this transition is normally forbidden by selection rules. For the absorption the situation is different, and only the A state, allowed by selection rules, can be excited [7]. Following this last remark three interesting observations can be made.

(i) The A line (observed in absorption) and B line (observed in luminescence) have nearly the same coupling with the lattice, while their angular momenta are different because the respective states have different symmetries. The same result holds for the A and B ZPL transitions of the exciton bound to iodine in AgBr [9], a host lattice with an indirect gap. Therefore, as it has been assumed by Testa *et al* [5], the phonons are preferentially coupled to the bound exciton as a whole, rather than to the more strongly bound particle as proposed in [7].

(ii) As already observed by Dietz *et al* [9], the absorption and luminescence spectra of ZnTe:O are nearly mirror images around the ZPL, i.e. the excited (or vibrational) states of the crystal ground state, seen in luminescence, and of the oxygen-bound-exciton state, seen in absorption, are the same, which can be described schematically in a configuration coordinate diagram. In contrast, in AgBr:I there is a difference of about one order of magnitude between the strength of the electron–phonon coupling in absorption and luminescence. This difference, which may be related to a relaxation process as discussed in [14], indicates that AgBr:I behaves as a deep impurity for emission and as a shallow one for absorption. For ZnTe:O no or nearly no relaxation is observed on the bound exciton and, therefore, ZnTe:O has to be considered as a deep impurity both for emission and for absorption.

(iii) The localization energy is large enough to separate the oxygen absorption spectrum almost completely from the shallow impurities and the free-exciton spectra.

The physical properties that determine the appearance of a relaxation effect are not yet well understood, and we give here only experimental evidence without any further interpretation.

### *3.2. Temperature dependence*

The temperature dependence of the luminescence spectrum of ZnTe:O has been calculated within the model of [5]. This approach is justified from the low-temperature results. We assume that there is no relaxation within the excited state and that the vibrational states are the same for the crystal ground state and for the oxygen-bound-exciton state. This assumption is reasonably confirmed by the experimental data and leads to theoretical spectra that are symmetric around the ZPL. The results of the fit for luminescence are presented in figure 3.

In figure 4 we present the luminescence and absorption spectra for different temperatures. The general features of the luminescence spectra are well described by the model in the temperature range between 2 K and 60 K. In particular, the slow disappearance of the phonon fine structure with increasing temperature is well reproduced. We also notice that the ZPL and the LO replica disappear more rapidly than the structure related to acoustical phonons. This feature is also well reproduced in spite of the imprecise fit of the relative peak strength. Furthermore, the spectra show the following features:

(i) the absorption and luminescence spectra are symmetric around the ZPL as predicted by the model;

(ii) the overlap between absorption and luminescence spectra is negligible over the whole range between low temperature and room temperature—we will comment on this point later on;

(iii) above 60 K a shift of the spectral position of the maximum of the luminescence intensity appears in figure 4.

From figure 5 we see that the maximum of the luminescence intensity has the same temperature dependence as the energy gap with a scaling factor for the energy. This shift in energy of the maximum of the luminescence intensity is essentially due to the natural shift in energy of the valence and conduction bands and we have introduced the measured shift into the fit. We therefore conclude that there is no detectable change in the Huang–Rhys factors with increasing temperature. Despite the imprecise fit of the relative peak intensities, this latter feature is nevertheless well reproduced by the model, as can be seen from figure 3.

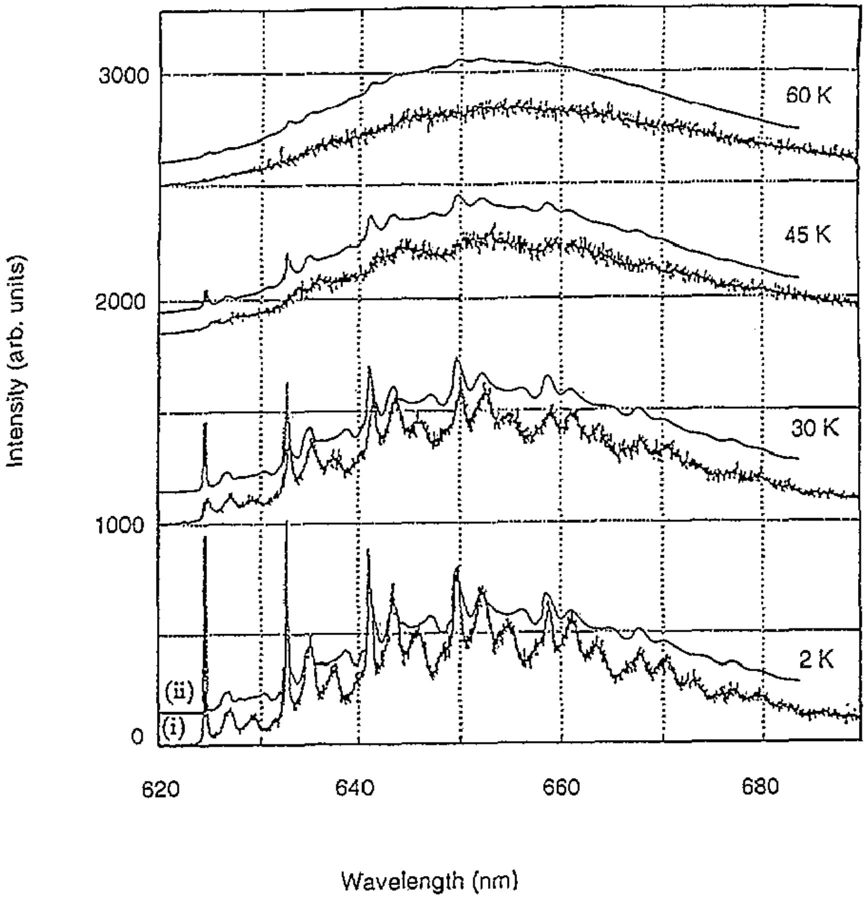


**Figure 3.** The fit (thin line (ii)) of the luminescence spectra (solid line (i)) for different temperatures.

Plotting the integrated intensity of the ZPL and of the LO replicas, figure 6 shows that they both follow the same exponential law $\sim e^{-\gamma T^2}$, where the experimental value for $\gamma$ is $\gamma_l \simeq 1 \times 10^{-3}\ K^{-2}$. This is in good agreement with the model [5] which predicts, based on multiphonon processes, that the total intensity of the ZPL and of the LO replicas follows a temperature behaviour given by

$$\int I \, dE \sim e^{-\gamma T^2}. \tag{3.1}$$

In this model equation (3.1) is obtained with the assumption that the acoustic phonons can be treated in a Debye assumption.

The same temperature dependence as that displayed in figure 6 has been found for the integrated absorption in [7]. In fact, the value $\gamma_l$ quoted above has been determined from absorption measurements and the few experimental points displayed in figure 6 show that it applies for luminescence as well. Moreover, it has been shown in [7] that the value of $\gamma_l$ is very close to that obtained by scaling the results for AgBr to ZnTe which is given by $\gamma_{scaled} = 0.8 \times 10^{-3}\ K^{-2}$. This agreement supports applicability of the approach of Testa *et al* [5] to isoelectronic traps.

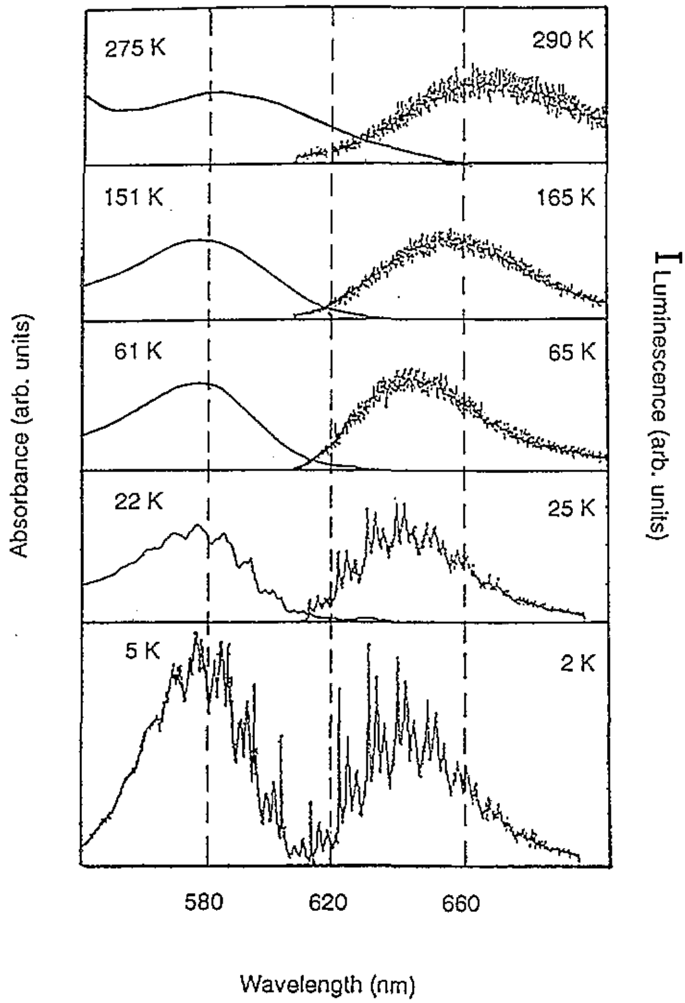


**Figure 4.** Luminescence and absorption spectra for different temperatures and normalized to each other with respect to the ZPL intensity for liquid helium temperature and to their maximum intensity for higher temperatures.

Moreover, at temperatures above 40–50 K, an exponential dependence of the integrated unstructured absorption is also expected [15], as shown in [7]. There we have found two different values for $\gamma$, $\gamma_2$ and $\gamma_3 \ll \gamma_1$. The change of the $\gamma$ factor of this unstructured absorption near 200 K could not be interpreted within the model and only experimental evidence is given.

In fact, the integrated luminescence of the unstructured part of the spectra behaves slightly in a more complicated way: for the *resonant excitation* case we fit the overall intensity with the same exponential dependence and with the same $\gamma_2$ and $\gamma_3$ as for absorption, and the agreement is rather good as can be seen from figure 7.

However, for *band-to-band excitation*, the overall temperature dependence of the intensity shows a different behaviour. The intensity decreases from liquid helium temperature to about 80 K and then increases up to room temperature, finally to reach the same efficiency as that at $\simeq$ 10 K as shown in figure 8. While for resonant excitation

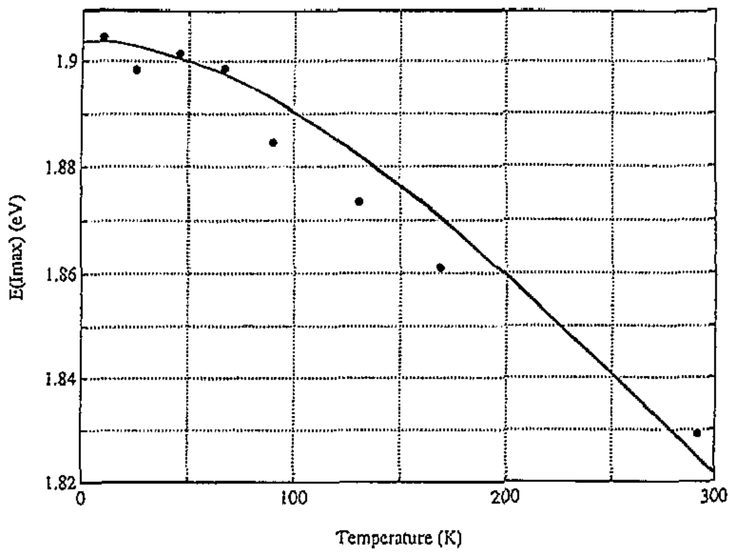


**Figure 5.** The maximum luminescence intensity as a function of temperature. The full line represents the scaled temperature variation of the gap in ZnTe [7].

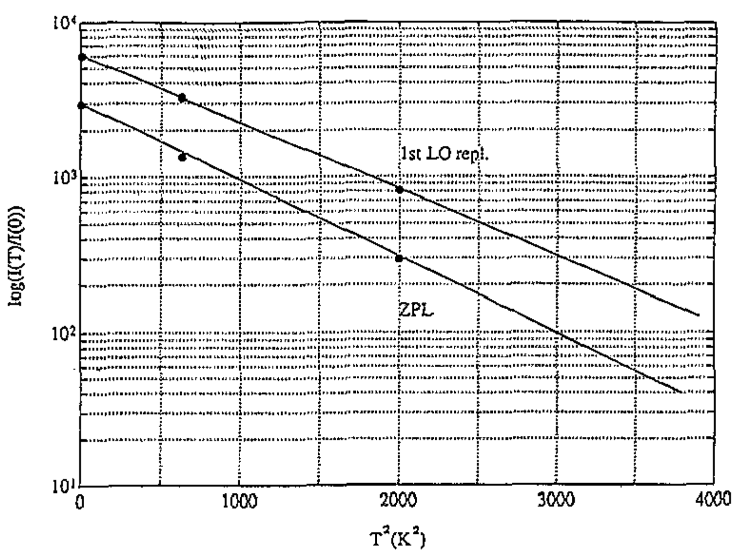


**Figure 6.** The temperature dependence of the integrated luminescence intensity of the ZPL and its first LO replica.

the luminescence intensity is directly related to the absorption coefficient, as borne out by the above results, the excitation within the conduction band is more difficult to analyse.

We add a few more general remarks.

(i) In the case of resonant excitation there is a symmetry between absorption and emission with respect to both the spectral shape and the temperature dependence. This

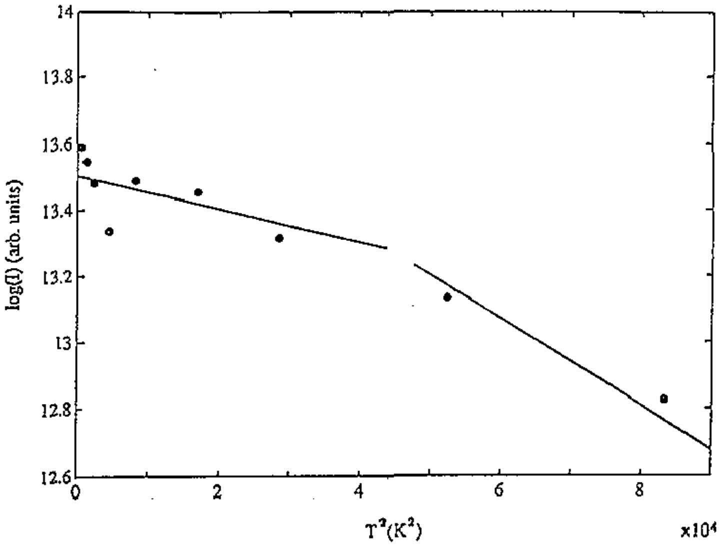


**Figure 7.** The temperature dependence of the overall luminescence intensity for resonant excitation. The points are fitted with (3.1) and with $\gamma_2 = 5.2 \times 10^{-6}\ K^{-2}$ and $\gamma_3 = 1.3 \times 10^{-5}\ K^{-2}$ determined in [7].

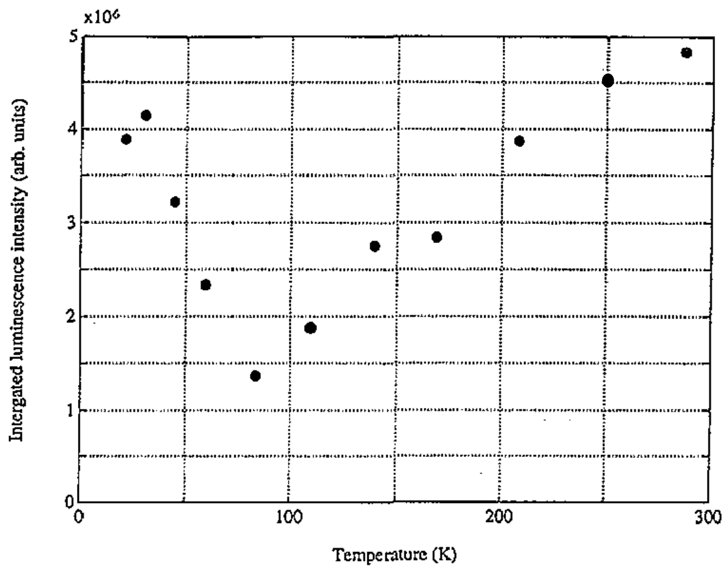


**Figure 8.** The temperature dependence of the integrated unstructured part of the luminescence spectra for band-to-band exciton.

means that the matrix element which appears in their expression is the same for both processes.

(ii) For band-to-band excitation the situation is not as clear-cut as in the resonant case. The symmetry between the emission and absorption spectra remains, but the temperature dependences for $T > 50$ K of the two processes differ.

(iii) The overlap between absorption and emission spectra remains negligible independently of the temperature as shown in figure 4. This feature is important in the context of gain prediction. The absence of absorption in the spectral range of luminescence indicates that an important gain may be expected, as has indeed been demonstrated in [1] and [2].

## 4. Luminescence decay time measurements

In the paper by Cuthbert *et al* [8] the bound-exciton lifetimes have been measured in the sample excited by an electron beam. We show in this section that the temperature dependence of these lifetimes strongly depends on the excitation energy.

Our results on the temperature dependence of these decay times are in good agreement with the results of [8] for band-to-band excitation, while in the case of resonant excitation a new behaviour appears with a steep jump in the lifetimes near 80 K.

We should like to stress here that with resonant excitation only the oxygen-bound exciton is excited while for band-to-band excitation we have to take into account the dynamics of the possible recombination path and trapping mechanisms of the charges involved. The results corresponding to different excitation and temperature regimes are presented in different subsections.

### *4.1. Low-temperature lifetimes*

For the low-temperature dependence of the bound-exciton lifetime, the experimental data basically agree with [8], particularly for the band-to-band excitation case. For resonant excitation the lifetimes are slightly smaller near 50 K and demand a generalization of the fitting formula which will be discussed now.

Having observed that in the low-temperature region all optical phonon replicas decay with the lifetime of the zero phonon A or B lines, the temperature dependence of this lifetime is related to the energetic splitting $\Delta E = 1.6$ meV and to the respective lifetimes $\tau_A$ and $\tau_B$. This dependence is governed by the thermalization between the two electronic states. Using the result from the model of Testa *et al* [5] that the interaction between optical and acoustical phonons gives a low temperature a reduction of the ZPL and optical-phonon-assisted transition probabilities by a factor of $e^{-\gamma T^2}$, we write

$$1/\tau = g_A N_A x_A/\tau_A + g_B N_B x_B/\tau_B \tag{4.1}$$

with $x_{A,B} = \exp(-\gamma_{A,B} T^2)$ and

$$\gamma_{A,B} = S_{A,B} \times \text{constant} \tag{4.2}$$

where $S_{A,B}$ are the Huang–Rhys factor (or coupling strengths) for the LO electron–phonon coupling with the A and B states respectively. All other quantities are defined as in [8] with the values $\tau_A = 9$ ns, $\tau_B = 318$ ns, $\Delta E = 1.6$ meV, and with

$$\begin{aligned} N_A/N_B &= e^{-\Delta E/kT} \\ g &= g_A/g_B = \tfrac{3}{5}. \end{aligned} \tag{4.3}$$

Finally, we find that

$$\tau = \frac{\tau_A\left(1 + g e^{-\Delta E/kT} e^{-(\gamma_A - \gamma_B)T^2}\right)}{\left((\tau_A/\tau_B) + g e^{-\Delta E/kT} e^{-(\gamma_A - \gamma_B)T^2}\right)}. \tag{4.4}$$

For a fit of the experimental data with (4.4) we use a value $\gamma_A - \gamma_B = -0.5 \times 10^{-3}\ K^{-2}$. This value is based on $\gamma_A = 1 \times 10^{-3}\ K^{-2}$ found in the last section and on estimated Huang–Rhys factors $S_A \simeq 2.5$ and $S_B \simeq 3$, which are based on the absorption and luminescence results at low temperature. The fit is shown in figure 9. Measuring the temperature next to the sample we assumed there was a systematic underestimation of the temperature of the excited volume of the sample and a shift of about 10 K was necessary to allow a fit with (4.4) to the experimental data. Comparing this fit to the one of Cuthbert and Thomas [8], the lower decay times found for high temperatures are determined by the additional factors $x_A$ and $x_B$ in (4.1). These low decay times could nevertheless not have been observed by Cuthbert and Thomas due to their limited time resolution.

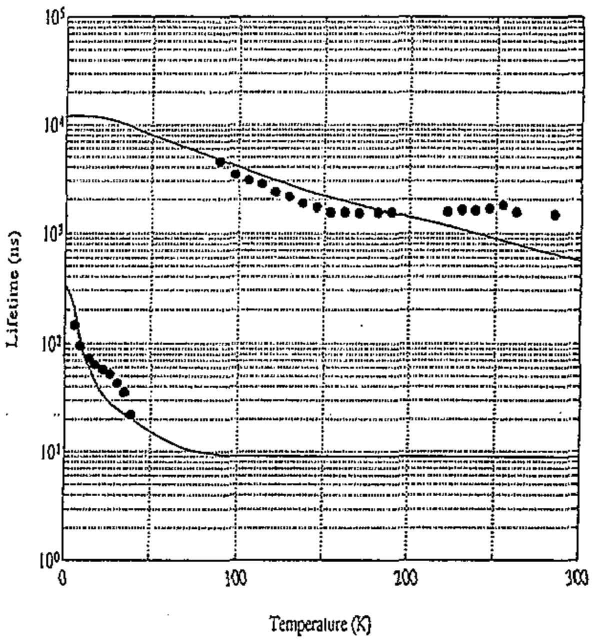


**Figure 9.** The temperature dependence of the experimental decay times (points) fitted with (4.4) with the values of the parameters quoted in the text for low temperatures, and with (4.5) for high temperatures.

## *4.2. High-temperature lifetimes for oxygen-resonant excitation*

According to the results presented in figure 9, we propose that the luminescence lifetimes of the oxygen-bound exciton are different for optical-phonon-assisted ($\tau_{short}$) and for the unstructured acoustical-phonon-assisted transitions ($\tau_{long}$). These features could be due to the limited wavevector of acoustical phonons which, according to the selection rules for a direct-gap semiconductor, would allow only emission of paired acoustic phonons. This could strongly lower the transition probability and consequently enhance the decay time. Furthermore, since there is an acoustic-phonon-assisted luminescence contribution for all temperatures, this implies the existence of a fast and slow decaying component also at low and medium temperatures ($T \leqslant 100$ K approximately). This is exactly the observation of Hjalmarson *et al* [16] who performed measurements in the frequency domain with a modulated electron beam for the excitation and who reported two decay times, $1/k_1$ and $1/k_2$, different by about two orders of magnitude, and with absolute values in good agreement with ours. However, in normal time-resolved experiments, a large difference between a fast and a slow component of decay times makes the detection of the *slower* decay very difficult.

In order to understand the slow component of the luminescence, we propose the following model: this luminescence emission is strongly acoustic-phonon-assisted and, furthermore, the emission of phonons is dominant with respect to phonon absorption up to 300 K in this process. The transition probability for phonon processes cannot be, therefore, expressed in terms of one-phonon processes and we have to consider the emission of two phonons with opposite $\boldsymbol{k}$-vectors satisfying the rule $k = 0$. These considerations lead to the following expression for the transition probability for phonon emission:

$$W \sim \left(n_q + 1\right)^2. \tag{4.5}$$

We take as the relevant acoustic phonon energies those that produce the first peak in the two-phonon density of states from [17]. The energetically higher LA mode is neglected. With $\tau \sim W^{-1}$ and using (4.5) we obtain

$$\tau = a\left(1 - 2\mathrm{e}^{-\alpha_1} + \mathrm{e}^{-2\alpha_1}\right). \tag{4.6}$$

A fit of (4.5) with $\alpha_1 = 7$ meV/$kT \simeq 90$ K/$T$ yields the curve shown in figure 9 where $a$ has been chosen to best fit the experimental points. Taking into account the particular simplicity of this model, the agreement is reasonable.

Finally, we should like to stress that for resonant excitation the lifetime observed represents the true recombination probability of the oxygen-bound exciton since no other impurities are excited.

## 5. High-temperature lifetimes for band-to-band excitation

When band-to-band excitation is performed, the lifetime of the excited oxygen traps has a temperature dependence that differs from the one presented in the former section. We relate this difference to the presence of acceptors in ZnTe:O. In the following we will indicate some interactions involving these acceptors that influence the temperature dependence of the lifetime of the excited oxygen traps.

The material ZnTe, either nominally pure or doped with oxygen, is known to have a number of residual impurities [18]. Among these impurities, Cu acceptors replacing Zn play an important role [18, 19]. In our samples, Cu acceptors were often found to be dominating [20]. First of all we have to be sure that an influence of the acceptors on the luminescence spectrum of the excited traps is present and is different for excitation above and below the band gap. A consequence of the presence of neutral acceptors, whose activation energy we call $E_A$, in uncontrolled concentrations of about $10^{+15}$–$10^{+16}$ cm$^3$ is the occurrence of so-called undulation spectra. These spectra yield a low energy tail of the ZPL of the bound

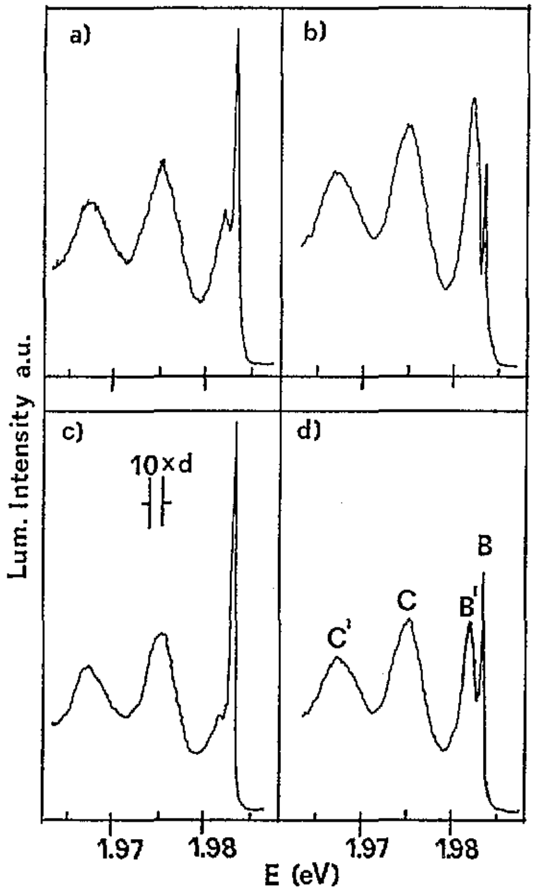


**Figure 10.** Undulation spectra related to the oxygen-bound exciton at 2 K. (a), (b) Higher Cu-acceptor concentration. (c), (d) Lower Cu-acceptor concentration. The curves in (a) and (c) correspond to band-to-band excitation with $E_x = 2.84$ eV; the curves in (b) and (d) correspond to resonant excitation with $E_x = 2.14$ eV, $E_g = 2.39$ eV. B indicates the bound-exciton ZPL, B′ the undulation spectrum, C, C′ the acoustic phonon replicas of the B ZPL.

exciton [11] and/or of the ZPL of excitons bound to intrinsic impurities. The latter case is well studied for GaP:N:Zn [11]. The presence of undulation spectra is a prerequisite for clarifying some aspects of the interaction of the isoelectronic trap oxygen with acceptors in ZnTe.

In figure 10 we show undulation spectra, which appear in the luminescence spectra of ZnTe:O for excitation energies $E_x$ above and below the band-gap energy $E_g$. The spectral shape of the luminescence is the same in both cases, except for the undulation tail of the ZPL and of its various LO phonon replicas. The undulation spectrum is not visible in absorption [7] because it is related to the properties of the interactions in the initial state of luminescence. These characteristics are in agreement with the known literature and are understood within the model of [11]. Following this model, pairs composed of isoelectronic impurity and a neutral acceptor bind an exciton with distance-dependent strength. The radiative decay of this exciton gives rise to the undulation spectra, which take some of the oscillator strength of the ZPL. In our case the intensity of the luminescence spectra is larger for excitation energies $E_x < E_g$, and acceptors are not excited, i.e. there are no excitons bound to them and they are neutral at low temperatures. This leads to optimal conditions for the strength of undulation spectra. In contrast, when exciting the sample via the gap, many acceptors will capture a bound exciton, or at least an electron which in a second step will capture a hole and thus complete a bound exciton. These acceptors are then not available for the formation of the oxygen–neutral-acceptor pair states which are responsible for the undulation spectra. Therefore, for $E_x > E_g$, the undulation spectra show systematically a smaller intensity than in the former case, as is observed in figure 10. These results indicate that there is a considerable influence of the concentration of neutral acceptors on the oxygen luminescence.

Besides the interaction leading to the undulation spectra, we propose a further mechanism of interaction between the isoelectronic trap oxygen and acceptors, which influences the temperature dependence of the lifetime of the excited oxygen trap: for both oxygen impurities and acceptors a finite probability exists that an electron is bound first. Therefore, a hole that is bound to the electron of one impurity of one type may diffuse to one of the other type and either recombine there or return to the first impurity. As we will show below, this process manifests itself in the temperature dependence of the lifetime. As we have seen above we qualitatively expect that this temperature dependence will be different for different excitation energies.

In order to give a quantitative discussion of this model we consider the process of ionization of the excitons bound to the oxygen and to the acceptor. Let $p_{\mathrm{O}}$ be the concentration of holes bound to the excitons of the oxygen trap and $p_{\mathrm{A}}$ that of the holes bound to the excitons of the neutral acceptor. Both concentrations $p_{\mathrm{O}}$ and $p_{\mathrm{A}}$, are defined without interaction between impurities such that their ratio $p_{\mathrm{O}}/p_{\mathrm{A}}$ is determined by the branching ratio of the respective recombination paths. These concentrations are now related through the rate equation

$$\partial p_{\mathrm{O}}/\partial t = g_{\mathrm{O}} - p_{\mathrm{O}}/\tau_{\mathrm{R_O}} - p_{\mathrm{O}}p_{\mathrm{A}}^{(\mathrm{e})}/f_{\mathrm{A}} + p_{\mathrm{O}}p_{\mathrm{A}}^{(\mathrm{e})}/f_{\mathrm{A}} \tag{5.1}$$

where $g_{\mathrm{O}}$ is the generation rate of oxygen-bound excitons and $(\tau_{\mathrm{R_O}})^{-1}$ is the inverse recombination time for these excitons. The remaining two terms describe the rate of the diffusion of holes from the oxygen trap to the acceptor and vice versa. On the acceptor they find electrons with a concentration $p_{\mathrm{A}}^{(\mathrm{e})}$. On the oxygen the inverse process involving the electron concentration $p_{\mathrm{O}}^{(\mathrm{e})}$ occurs. For $p_{\mathrm{A}}$ too, a rate equation holds:

$$\partial p_{\mathrm{A}}/\partial t = g_{\mathrm{A}} - p_{\mathrm{A}}/\tau_{\mathrm{R_A}} - p_{\mathrm{A}}p_{\mathrm{O}}^{(\mathrm{e})}/f_{\mathrm{A}} + p_{\mathrm{O}}p_{\mathrm{A}}^{(\mathrm{e})}/f_{\mathrm{A}}. \tag{5.2}$$

In the stationary regime, and after elimination of $g_{\mathrm{A}}$, and having expressed $g_{\mathrm{O}}$ in the limit $1/f_{\mathrm{A}} = 0$, $1/f'_{\mathrm{A}} = 0$ when the acceptors have no influence (as for resonant excitation), i.e. $N_{\mathrm{A}} = 0$, we get

$$\left(1/\tau_{\mathrm{R_O}}\right)\big|_{\mathrm{eff}} = \left(1/\tau_{\mathrm{R_O}}\right)\big|_{N_{\mathrm{A}}=0}\left(1 - p_{\mathrm{A}}\mathrm{e}^{-W_{\mathrm{A}}/kT}\tau_{\mathrm{R_O}}\left(1/f_{\mathrm{A}} - 1/f'_{\mathrm{A}}\right)\right). \tag{5.3}$$

Here thermal equilibrium between the concentrations of bound excitons of the oxygen trap as well as those of the acceptor and the respective ionized species has been assumed, i.e.

$$\begin{aligned} p_{\mathrm{O}}(\mathrm{e}) &= p_{\mathrm{O}}\mathrm{e}^{W_{\mathrm{O}}/kT} \\ p_{\mathrm{A}}(\mathrm{e}) &= p_{\mathrm{A}}\mathrm{e}^{-W_{\mathrm{A}}/kT}. \end{aligned} \tag{5.4}$$

In this expression the ionization energies $W_O$ and $W_A$ of oxygen- and acceptor-bound excitons have been introduced with the value $W_A \simeq W_{FE} = 13$ meV respectively [18], $W_{FE}$ being the free-exciton binding energy. The quantity $W_O$ is a free parameter to be determined by fitting the experimental data. The choice of the value for $W_A$ is justified from the low localization energy of the Cu-bound exciton which is of 6 meV only [18]. Similar values for hold for most acceptors [18].

The capture cross sections $1/f_A$ and $1/f'_A$ have to be temperature dependent. In order to account for their temperature dependence we make the following assumptions: the acceptor-bound excitons are approximately free and are, therefore, described in the effective-mass approximation as hydrogen-like excitons. The cross section for the capture of an electron of energy $E$ by a proton is found to vary nearly as $E^{-1}$ for sufficiently low energies [21], i.e. as $E \ll E_{Ryd}$. We modify this result for our purpose by identifying $E$ with $kT \ll W_A$ at low temperature. Therefore, the capture cross section via Coulomb forces is approximately given by $W_A/kT$. At higher temperatures capture of an electron by pure Coulomb forces is practically impossible due to the kinetic energy of the charge carriers. However, the interaction with acoustic phonons in a crystal is very effective in reducing the kinetic energy of charge carriers, as is known from the elementary theory of electronic conduction. Thus we account for the capture rate at higher temperatures by adding to the capture cross section a term $\nu kT/k\theta$ with an average value of the Debye temperature $\theta = 250$ K for ZnTe:O and an adjustable parameter $\nu$. Finally we choose the capture cross section of the much stronger localized oxygen-bound exciton to be equal to one. Therefore, we get

$$\begin{aligned} 1/f_A &= W_A/kT + \nu kT/k\theta \\ 1/f'_A &= 1. \end{aligned} \tag{5.5}$$

The relaxation time is then expressed as

$$\begin{aligned} \tau_{R_O} &= \tau_{R_O}\big|_{N_A=0}\Big[1 - A e^{-W_A/kT}\big(W_A/kT + \nu kT/k\theta - e^{\Delta/kT}\big)\Big]^{-1} \\ A &= p_A \tau_{R_O} \end{aligned} \tag{5.6}$$

where $\Delta = W_O - W_A$, and $p_A\tau_{R_O}$ and $\nu$ are free parameters whose values are fixed by fitting the experimental data. The result of the fit for the following values of the fit parameters $\Delta = 2.4146$ meV, $\nu = 0.143$, $W_O = 137$ meV is presented in figure 11 and appears to be quite satisfactory.

The expression (5.6) for the lifetime $\tau_{R_O}$ is not valid for arbitrary temperatures because it diverges for $T$-values much larger than 300 K. As we know from the experiments [8], for temperatures larger than 300 K the lifetime rapidly decreases as a consequence of the thermal release of the bound excitons as a whole. This process has not been included in our considerations and its absence indicates the limits of our model. Within this description the temperature dependence of the lifetime for oxygen-bound-exciton recombination when the excitation is above the band gap reduces to the one obtained for resonant excitation multiplied by a term that includes the effect of the interaction between oxygen-bound and acceptor-bound excitons. This last interaction is only relevant for excitation above the band gap as indicated by the weak intensity of the undulation spectra.

We conclude by giving two more arguments in favour of our description. One of the fitting parameters, namely the energy $W_O$, has a value of $140 \pm 50$ meV, which is a large value but not unreasonably high [22]. Finally we have also fitted the data of [8] using the same fitting parameter values as in figure 11, with a value of $(\tau_R)^{-1}$ for $N_A = 0$ which is obtained from the (4.4). The fit that is presented in figure 12 is once more very satisfactory.

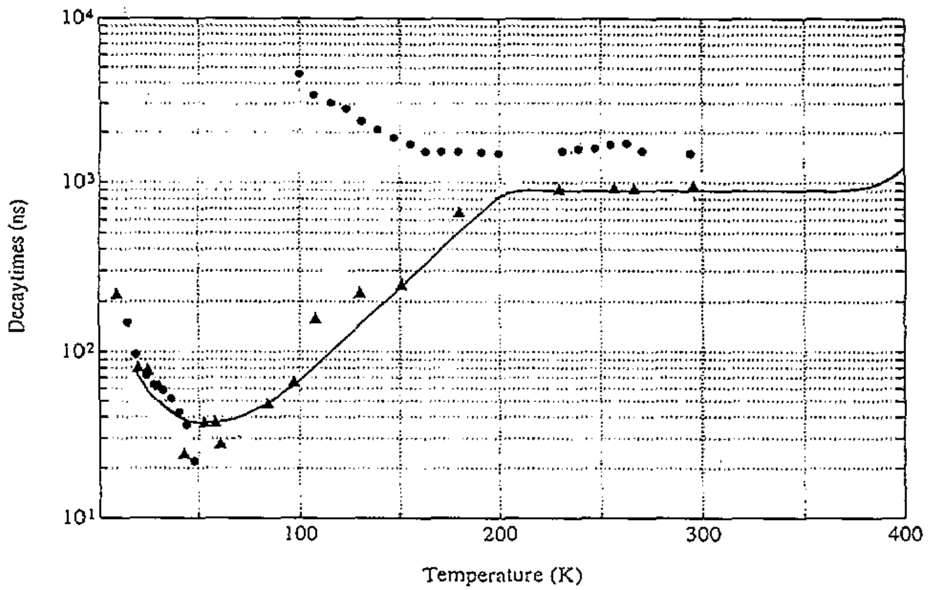


**Figure 11.** Decay times for the oxygen emission at the maximum of the intensity for resonant excitation (●●●) and Band-to-band excitation (▲▲▲). The solid line shows the result of a fit to (5.6) with parameter values $\Delta = 2.4146$ meV, $\nu = 0.143$ $W_O = 137$ meV.

## 6. Conclusions

The experimental results and their interpretations presented so far allow a better understanding of the emission properties of ZnTe:O and confirm the results obtained from the gain spectra [1,2].

The behaviour of the luminescence from ZnTe:O for low temperature is similar to that of AgBr:I in different respects, as for example in what concerns the temperature dependence of the spectra. The luminescence from both isoelectronic impurities is well described in terms of the model of [5]. Therefore, this model seems to be quite useful for describing the optical properties of isoelectronic traps in different materials. Furthermore, the experimental results on luminescence match well with that obtained for absorption presented in [7] with the results for the gain [27] for resonant as well as for band-to-band excitation.

For higher temperatures we have succeeded in giving a satisfactory description of the luminescence spectra, which once more coincide with the gain spectra [1,2]. Furthermore, we have presented results on the temperature dependence of the relaxation times at low temperature, which complete those given in [8]. We have also been able to give a reasonable fit of the experimental results for the temperature dependence of the relaxation time for band-to-band excitation in terms of a phenomenological model that accounts for the influence of acceptors in ZnTe on the relaxation times. For resonant excitation we have given a plausible fit of this temperature dependence by introducing the effect of two-phonon transitions. The influence of these transistors and of the two-phonon density of states on the emission characteristics has not been studied in detail in this paper and is left as a subject for future investigation.

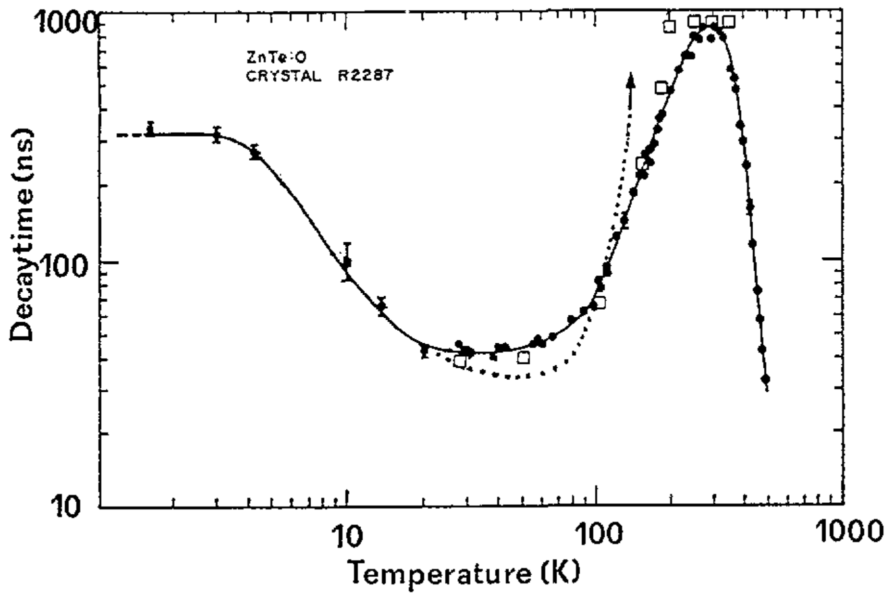


**Figure 12.** Luminescence decay time versus temperature (points) from [8]. The full line is a guide to the eye from 15 K on. The excitation of the sample is performed with an electron pulse of energy $\gg E_g$ and width of $30 \times 10^{-9}$ s with an intensity of $10^{-4}$ A cm$^{-2}$. The dotted line gives the fit to $\tau_{eff} = \tau(T)(1 - \phi \exp(-\varepsilon/kT))^{-1}$ with $\phi = 1.7$ and $\varepsilon = 5.7$ meV from [8]. The points marked ■■■ were fitted to (5.6) with the parameters of figure 11. Both fits use $\tau(T)$ from (4.4) because of the limited time resolution in [8].

## Acknowledgments

We thank J W Allen for helpful discussions and H Berger for growing the crystals of ZnTe. One of us (YB) acknowledges support by the Fonds National Suisse.

## References

[1] Burki Y, Schwendimann P, Czaja W and Berger H 1990 *Europhys. Lett.* **13** 555
[2] Burki Y, Schwendimann P, Czaja W and Capozzi V 1991 *Europhys. Lett.* **16** 763
[3] Schwendimann P, Sigmund E and Zeile K 1988 *Phys. Rev.* A **37** 3018
[4] Schwendimann P and Burki Y 1992 *Phys. Rev.* B **46** 7479
[5] Testa A, Czaja W, Quattropani A and Schwendimann P 1987 *J. Phys. C: Solid State Phys.* **20** 1253
[6] Testa A, Czaja W, Quattropani A and Schwendimann P 1988 *J. Phys. C: Solid State Phys.* **21** 2189
[7] Slusarenko V, Burki Y, Czaja W and Berger H 1990 *Phys. Status Solidi* b **161** 897
[8] Cuthbert J D and Thomas D G 1967 *Phys. Rev.* **154** 763
[9] Dietz R E, Thomas D G and Hopfield J J 1962 *Phys. Rev. Lett.* **8** 391
[10] Hjalmarson H P, Hones E D and Norris C B 1987 *Solid State Commun.* **61** 555
[11] Dean P J and White A M 1976 *Solid State Electron.* **21** 1351
Street R A and Wiesner P J 1976 *Phys. Rev.* B **14** 632
[12] Marquis F 1984 *Thèse de Diplôme en Physique Théorique* EPFL, Lausanne, Switzerland
[13] Hopfield J J, Thomas D G and Lynch R T 1966 *Phys. Rev. Lett.* **17** 512
[14] Burki Y and Czaja W 1989 *Europhys. Lett.* **10** 55
[15] Maradudin A A 1966 *Solid State Physics* vol 18 (New York: Academic) p 406
[16] Hjalmarson H P and Norris C B 1987 *J. Appl. Phys.* **61** 734
[17] Plumelle P and Vandevyver M 1976 *Phys. Status Solidi* b **78** 271

[18] Venghaus H and Dean P G 1987 *Phys. Rev.* B 21 1596
[19] Mangea N, Molva E, Bensahel D and Romestein R 1980 *Phys. Rev.* B 22 2983
[20] Burki Y 1992 *Thèse de Doctorat No 991* Départment de Physique, EPFL, Lausanne, Switzerland
[21] Massey H S M and Burhop E H S 1952 *Electronic and Ionic Impact Phenomena* (Oxford: Clarendon) p 332
[22] Allen J W 1993 Private communication (University of St Andrews, UK)
With respect to the hole binding energy, ZnTe:O with the bound exciton may be considered in a reasonable approximation as an acceptor. The electronic effective mass binding energy for acceptors is 87 meV. Acceptor activation energies are found experimentally in ZnTe:O to be in the range from 60 meV to 150 meV as shown e.g. in
Venghaus H and Dean P G 1987 *Phys. Rev.* B 21 1596
The value found in our case for the isoelectronic trap therefore appears reasonable.